NATIONAL BUREAU OF STANDARDS
MICROCOPY RESOLUTION TEST CHART

| REPORT DOCUMENTATION PAGE | READ INSTRUCTIONS BEFORE COMPLETING FORM |
|---|---|

| 1. REPORT NUMBER | 2. GOVT ACCESSION NO. | 3. RECIPIENT'S CATALOG NUMBER |
|---|---|---|
| 14673.1-R-E | | |

| 4. TITLE (and Subtitle) | 5. TYPE OF REPORT & PERIOD COVERED |
|---|---|
| An Investigation of High Pressure Gaseous injections into Liquid Propellants | Final Report 1 Jan 77 - 28 Feb 78 |
| | 6. PERFORMING ORG. REPORT NUMBER |

| 7. AUTHOR(s) | 8. CONTRACT OR GRANT NUMBER(s) |
|---|---|
| C. R. Wimberly | DAA G29-77-G-0050 |

| 9. PERFORMING ORGANIZATION NAME AND ADDRESS | 10. PROGRAM ELEMENT, PROJECT, TASK AREA & WORK UNIT NUMBERS |
|---|---|
| The University of Mississippi University, Mississippi 38677 | |

| 11. CONTROLLING OFFICE NAME AND ADDRESS | 12. REPORT DATE |
|---|---|
| U. S. Army Research Office Post Office Box 12211 Research Triangle Park, NC 27709 | 1 May 78 |
| | 13. NUMBER OF PAGES 49 P. |

| 14. MONITORING AGENCY NAME & ADDRESS(if different from Controlling Office) | 15. SECURITY CLASS. (of this report) |
|---|---|
| | Unclassified |
| | 15a. DECLASSIFICATION/DOWNGRADING SCHEDULE NA |

16. DISTRIBUTION STATEMENT (of this Report)

Approved for public release; distribution unlimited.

17. DISTRIBUTION STATEMENT (of the abstract entered in Block 20, if different from Report)

NA

18. SUPPLEMENTARY NOTES

The findings in this report are not to be construed as an official Department of the Army position, unless so designated by other authorized documents.

19. KEY WORDS (Continue on reverse side if necessary and identify by block number)

20. ABSTRACT (Continue on reverse side if necessary and identify by block number)

It has been recognized for many years that liquid propellants (LP) offer several advantages over solid propellants when applied to guns. One of the concerns has been the repeatability of the pressure-time curves in the chamber, and occasional high pressure values that could exceed design limits of the casing. It is apparent that several variables may be involved and that the LP is extremely sensitive to small changes in conditions at ignition and in the LP chamber. It was the attempt of the work reported here to provide more information on the ignition phase of the LP gun system operation. Simulation of the penetration sequence for gaseous injections into

DD FORM 1473 EDITION OF 1 NOV 65 IS OBSOLETE

14673.1-R-E

20. ABSTRACT CONTINUED

liquid propellants provided greater understanding of the significance of
geometry and flow conditions on gas bubble formation, penetration depth and
rate.  Comparisons of test data and a simulation model indicated that the
model is good to excellent in predicting the penetration depth and rate of the
injection for the first 500 microseconds.  The shape of the bubble obtained
experimentally approached closely a prolate spheroid.

14673.1-R-E

An Investigation of High Pressure Gaseous

Injections into Liquid Propellants


Final Technical Report



by

C.R. Wimberly

The University of Mississippi

D D C

RECEIVED

JUN 27 1978

E

## Forward

This document is the final report of the basic research project
(P-14673-R-E) entitled "An Investigation of High Pressure Gaseous
Injections into Liquid Propellants" granted by the U.S. Army
Research Office (Grant number DAA G29-77-G-0050) for a 12-month post
LRCP study from 1 January 1977 to 31 December, 1977. A 90 day no-
cost extension was obtained in December to allow completion of
laboratory experiments that were completed on or about 31 March 1978.

Table of Contents

## List of Illustrations

## Introduction

It has been recognized for many years that liquid propellants (LP) offer several advantages over solid propellants when applied to guns (References 1 through 8). Advantages which have become generally accepted include elimination of the cartridge case, high loading densities, reduced storage requirements, vulnerability reduction and increased flexibility in vehicle design due to weight and volume redistribution.[9] Because of these advantages much research and hardware development has been done at the BRL and at other places, including extensive test programs, which have in turn uncovered several problem areas. One of the concerns over the years has been the repeatibility of the pressure-time curves in the chamber, and occasional high pressure values that could exceed design limits of the casing.[10] It is apparent that several variables may be involved and that the liquid propellant is extremely sensitive to small changes in conditions at ignition and in the LP chamber. It was the attempt of this work reported here to provide more information on the ignition phase of the LP gun system operation.

The pyrotechnic igniter, which exhausts hot, high pressure gases into the LP is considered the prime candidate for causing variations in propellant decomposition, since it has not been greatly controlled in the past. The igniter itself is a solid capsule upstream of an orifice that decomposes very rapidly, sending the products of combustion through the orifice into the liquid propellant. These products are known and the conditions at injection are somewhat controlled. The phase of ignition that is very crucial and one that needs further investigation is the moment the gases exit the orifice, the subsequent

1

penetration until propellant ingition.  From tests, this important phase
of ignition lasts about 500 microseconds.  But, during this time, the
gas bubble has penetrated the liquid by several centimeters, and the
shape and surface area have been developed which dictates decomposition
rate.  High pressures occur in the chamber during this period and it
has been observed that the gases shear the liquid into many droplets.
It is important to understand the conditions of the bubble at the
instant of ignition of the LP because of its affect on the decompo-
sition rate and therefore pressure variations with time in the chamber.

Experimentally, an apparatus was used to provide high igniter
chamber pressures and several orifice designs to investigate the
effects on control of the injection.  A high speed camera (on loan
from the BRL) was used to provide a visual determination of the gas
bubble formation, penetration depth and rate, gas-liquid entrainment
and shock wave propagation.  Tests were run to determine the sensitivity
and effects of geometry (orifice size and shape), upstream initiation
pressure, and the repeatability of tests.

Analytically, the gas bubble formation was mathematically
modeled to simulate the sequence of events as the high pressure gaseous
products penetrates the liquid propellant.  The model includes the gas
bubble formation, gas-liquid interactions, penetration depth and rate,
plus the effects of pressure waves.

## Analytical Effort

The mathematical model developed under the grant consists of two separate models, 1) a simple model based on the equations of state of the gas and liquid, which will be designated Model I, and 2) a more sophisticated model based on linear continuity and the momentum equations (Model II). Model I utilizes estimates of the gas volume as a function of time, while Model II predicts the bubble shape, pressure, velocity distribution, and densities as functions of time and distance downstream in the chamber. References 12 through 16 were helpful in these developments.

The basic volume equation for Model I is

$$V_o = V_g + V_L$$

where $V_g$ is the volume of the gas and $V_L$ is the volume of the liquid. The volume of the gas is calculated using the real gas equation of state and the compressibility factor, Z, because of the high pressures involved. The volume of the liquid is expressed in terms of the bulk modulus, which is assumed to vary linearly with the pressure. Assuming choked flow and a constant mass flow into the chamber, the mass of the gas is known as a function of time. Equation (1) is then solved numerically for the chamber pressure at any time, t.

If the effect of the pressure wave is neglected, $V_o$ is the total volume behind the wave front as it moves downstream and in front of the wave as it reflects from the far end of the chamber.

In Model I the shape of the gas bubble is assumed to be a prolate spheroid with various ratios of major diameters (see Figure 1). The

proper ratio will be estimated from experimental results.

In Model II, the variable x is the distance downstream in the chamber and t is the time. It is desired to determine r, the radius of the bubble, as a function of x and t. Other quantities currently determined include velocities, pressure, and densities. The velocity is assumed parabolic over the cross section. This results in four velocity parameters (two for the gas and two for the liquid) which vary with x and t. The pressure and densities of the liquid and gas are also assumed to vary with x and t alone. The boundary of the liquid and gas is currently assumed perfect with no mixing, vapor pressure, or gas bubbles. The temperature is assumed constant throughout the chamber and for the length of the time considered.

For the eight dependent variables mentioned above, eight equations are needed. These consist of the state, continuity, and momentum equations for both the gas and the liquid, plus two boundary conditions at the gas-liquid interface.

Taking a volume element of width dx, the unsteady continuity equation can be derived which results in the following equation (see Figure 1).

$$\rho \frac{\partial A}{\partial t} + A \frac{\partial \rho}{\partial t} + \rho U_b \frac{A}{x} + \quad (\rho \frac{\partial U}{\partial x} + U \frac{\partial \rho}{\partial x}) \, dA = 0$$

Here, $\rho$ is density, A is cross sectional area, U is velocity and $U_b$ is velocity at the boundary. Considering a momentum analysis of the same element under unsteady flow conditions produces

$$-A \frac{\partial p}{\partial x} - 2\pi r \mu \left[ \frac{\partial u}{\partial \xi} \right]_{\xi=r} = \rho U_b \left( \frac{\partial A}{\partial t} + U_b \frac{\partial A}{\partial x} \right)$$

$$+ \quad (\rho \frac{\partial U}{\partial t} + 2\rho U \frac{\partial U}{\partial x} + U \frac{\partial \rho}{\partial t} + U^2 \frac{\partial \rho}{\partial x}) \, dA$$

Here, $\rho$ is pressure $\mu$ is viscosity, and $\xi$ is the radial coordinate.

Substituting the assumed parabolic velocity distribution into equations (2) and (3) for both the gas and the liquid gives four partial differential equations. Two additional equations are obtained from equations of state.

For the gas

$$p = \rho RTZ$$

and for the liquid

$$\beta = \frac{-dp}{dv/v}$$

where the bulk modulus, $\beta$, is assumed to vary linearly with pressure. Two additonal equations are obtained by making the velocity and shear stress continuous at the gas-liquid boundary. Suitable initial conditions and boundary conditions at the entrance to the chamber complete the formulation of the problem.

The system of eight equations described above are highly nonlinear, first-order partial differential equations. To solve these, the method of lines was employed.[17] First, finite differences with respect to t were taken, producing a set of eight ordinary equations in terms of the independent bariable x. There equations were then solved by a standard Runge-Kutta technique. The resulting penetration depth and rate are shown in Figures 2 through 9.

The model currently assumes negligible gas-liquid entrainment, and temperature variations. It also does not provide for radial pressure waves or the effects of solid particles that may be injected into the LP. The model exhibits a particular problem of x=o. The solution is sensitive to the gas velocity of the entrance and an idealized model gives a singularity of the gas-liquid interface at x=o.

In Model II, the shape of the bubble remains almost cylindrical in shape as x and t vary. In order to more accurately predict the shape of the bubble, it is believed that the momentum equation in the radial direction should be considered in addition to the equations already used. This involves introducing a radial velocity component. In order to maintain x and t as the only independent variables, the momentum equation in the radial direction will have to be integrated with respect to the radial coordinate, $\xi$. This could be accomplished by assuming a distribution of the radial velocity component over the cross section, leaving certain parameters as functions of x and t. At the gas-liquid interface, the radial velocity component will be equal to the time derivative of r.

Inclusion of the pressure wave was obtained into the model via the momentum equations, which were integrated in the x-direction in the usual Runge-Kutta fashion. If the wave front was encountered, the pressure change across the front was taken into account. This phenomenon was primarily encountered between 125 and 250 micro-seconds when the wave front was again traveling downstream.
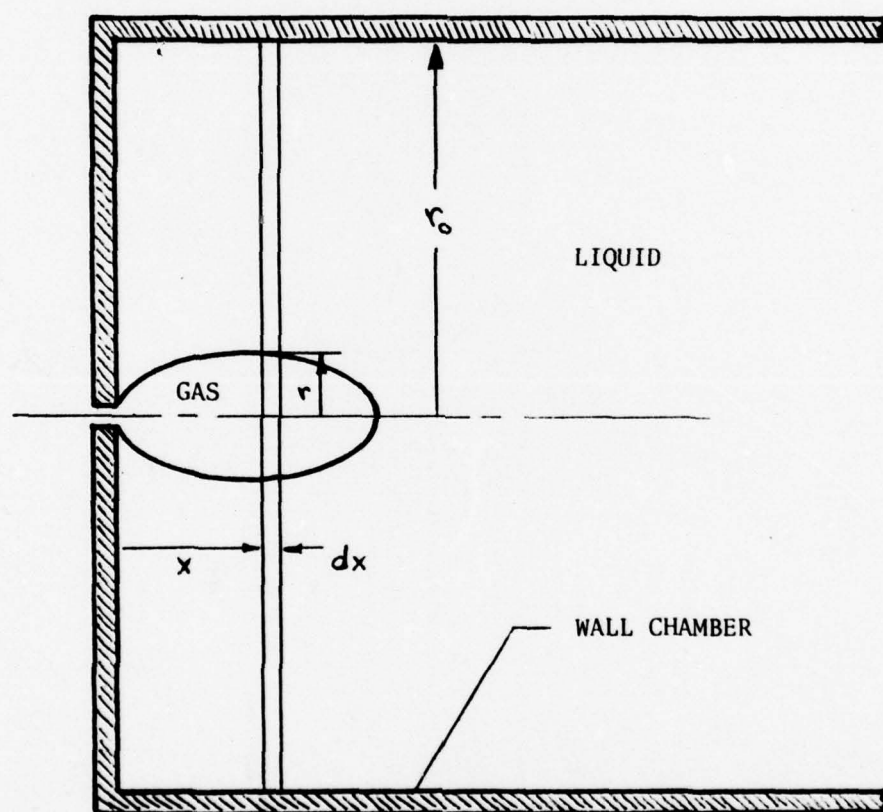
Figure 1. Coordinates and sketch of Gas Bubble -
Liquid Chamber Relation
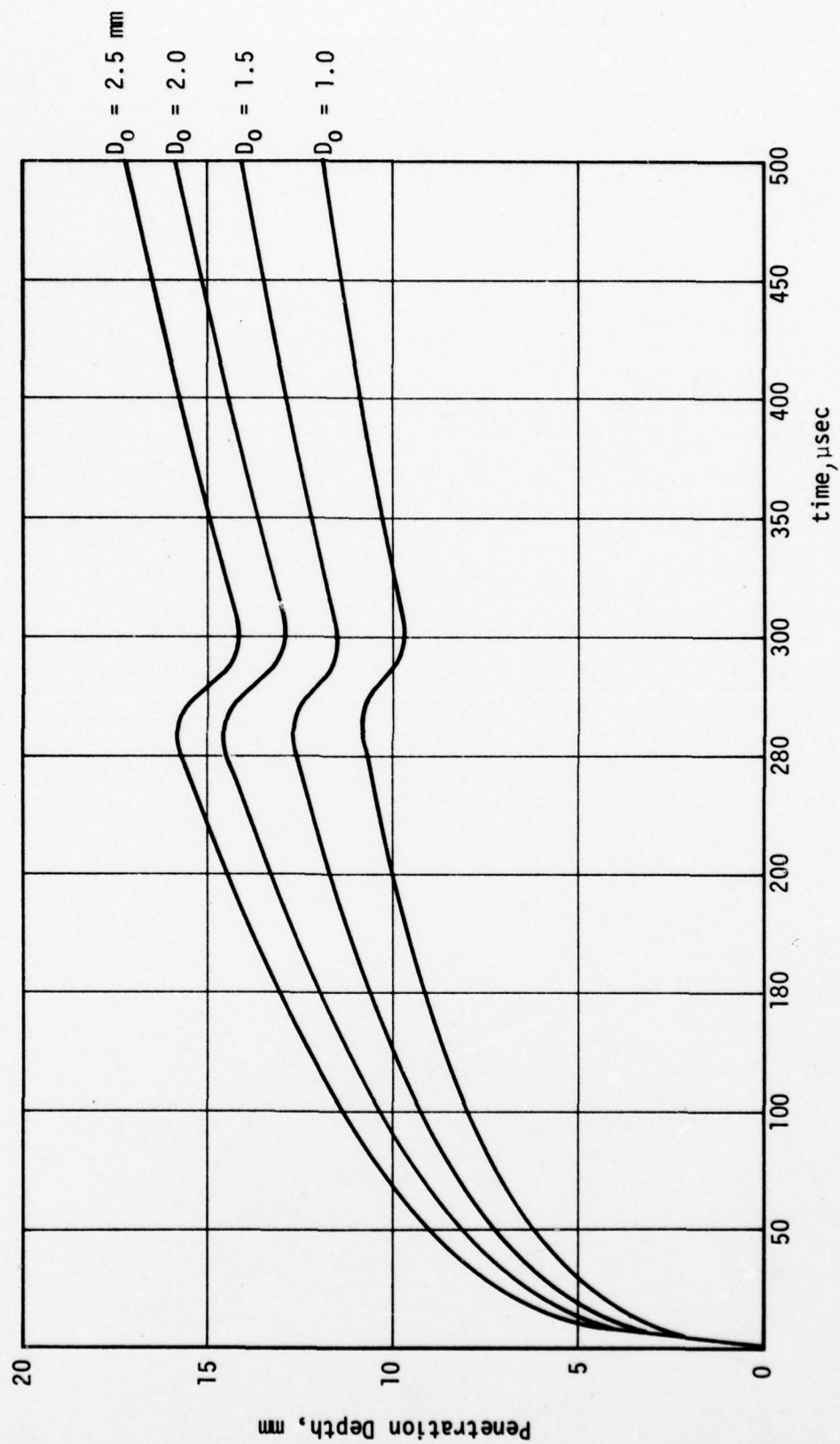
Figure 2.  Penetration Depth vs. Time, $\gamma = 1.4$, $T_0 = 294°K$

8

Figure 3. Penetration Depth vs. Time, $\gamma = 1.4$, $T_0 = 1000°K$

9
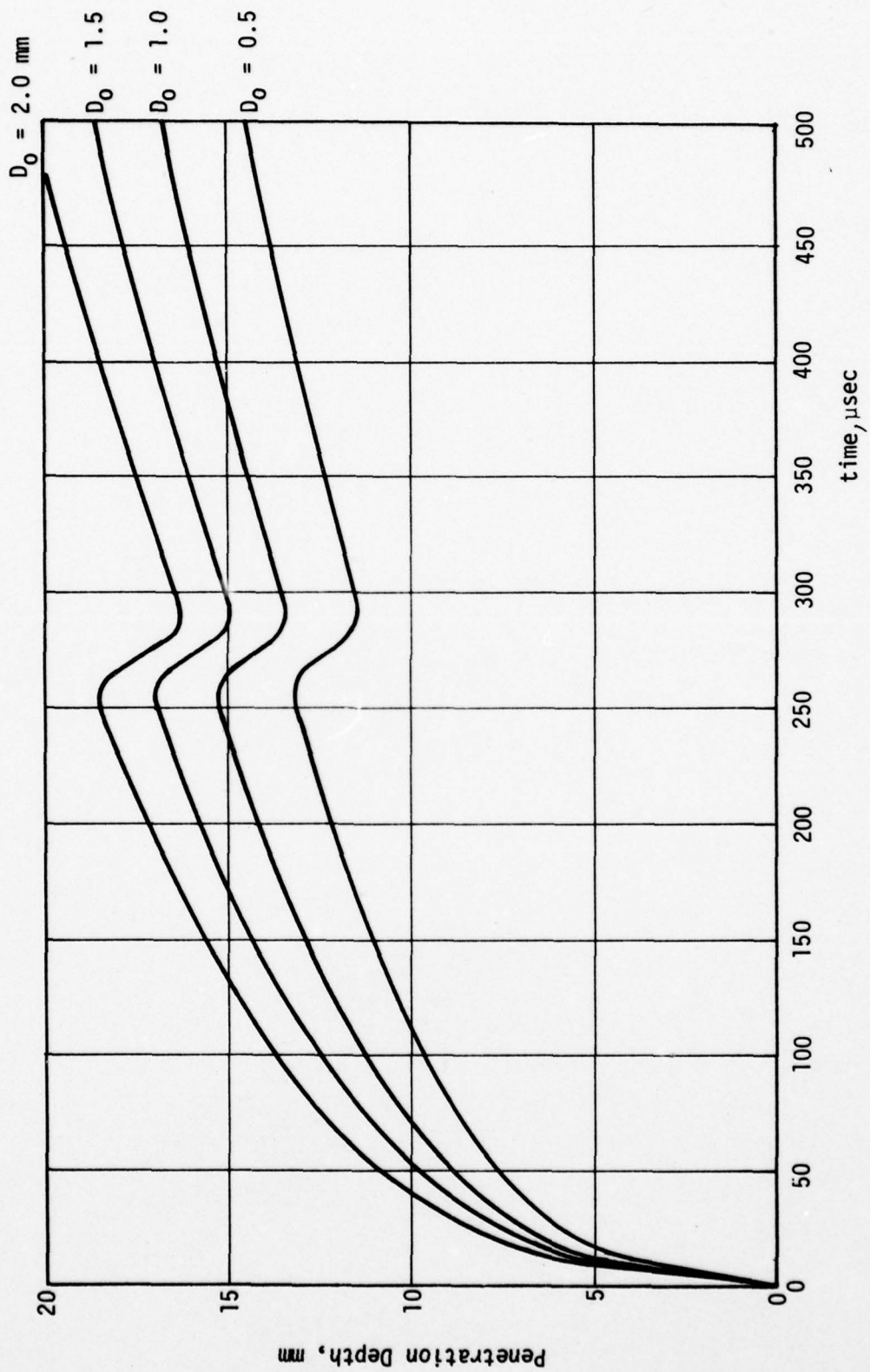
Figure 4. Penetration Depth vs. Time, $\gamma = 1.2$, $T_o = 1000°K$
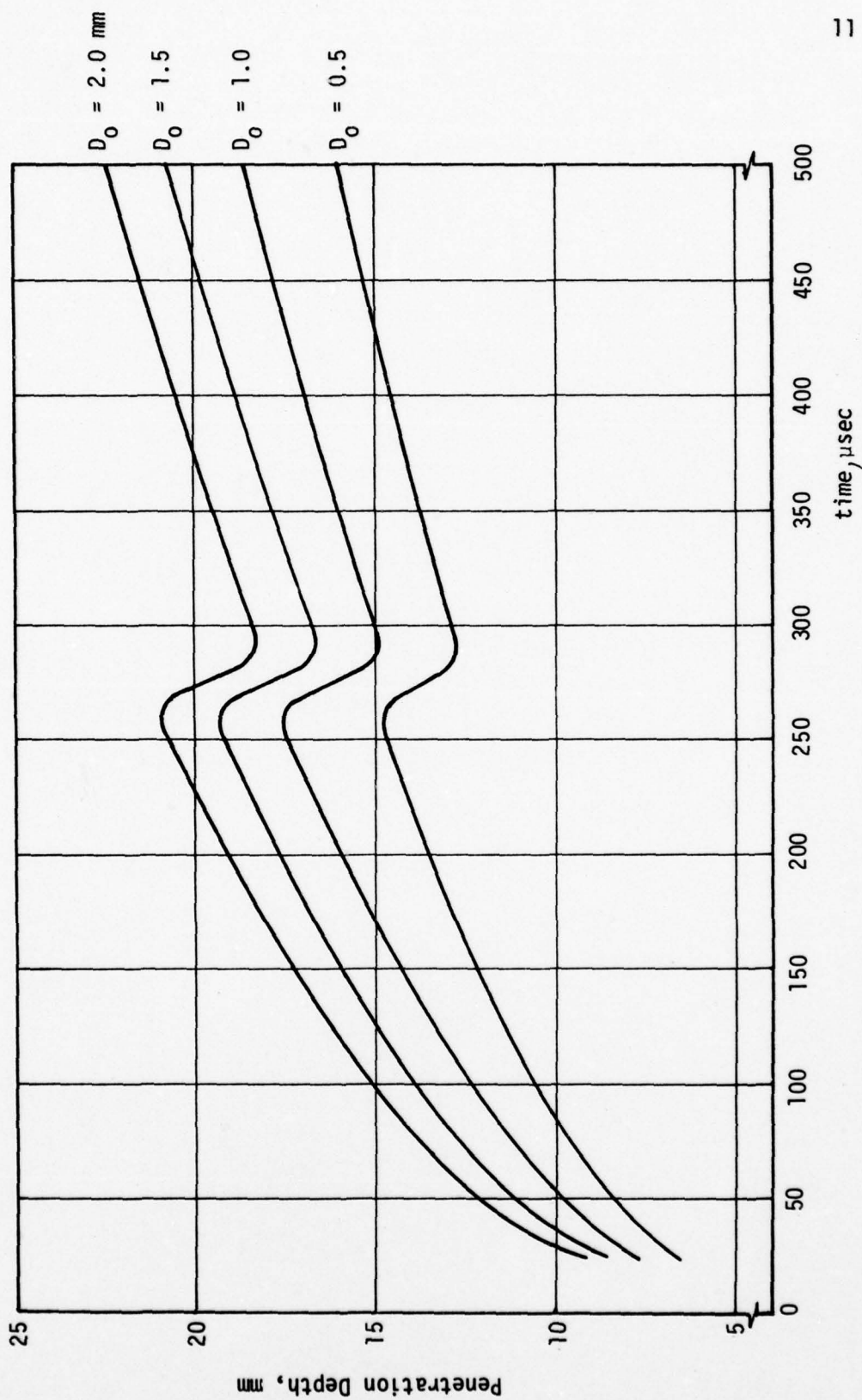
Figure 5.  Penetration Depth vs. Time, $\gamma = 1.2$, $T_0$ 3000°K

11
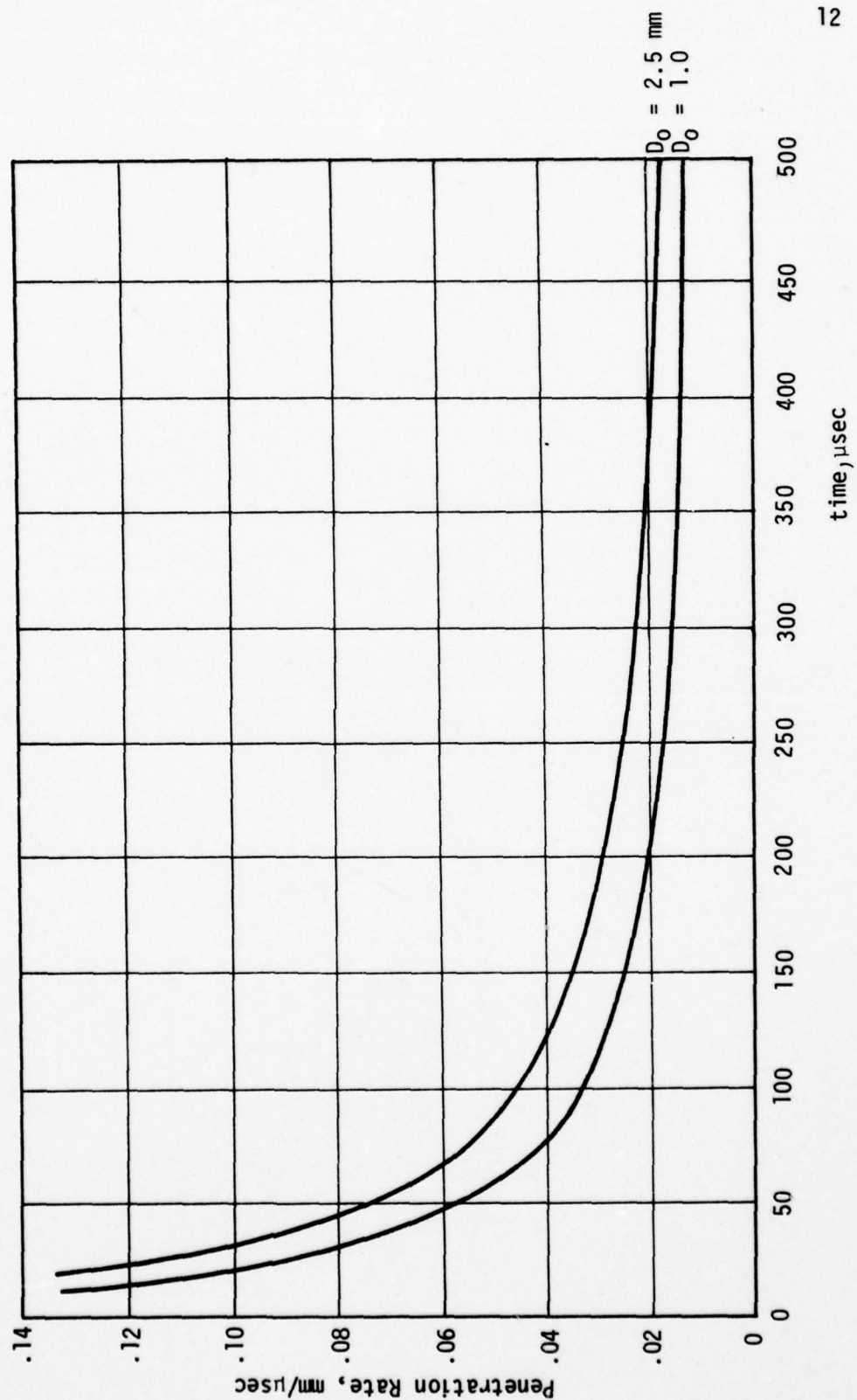
Figure 6.   Penetration Rate vs. Time, $\gamma = 1.2$,
$T_o = 1000°K$

12
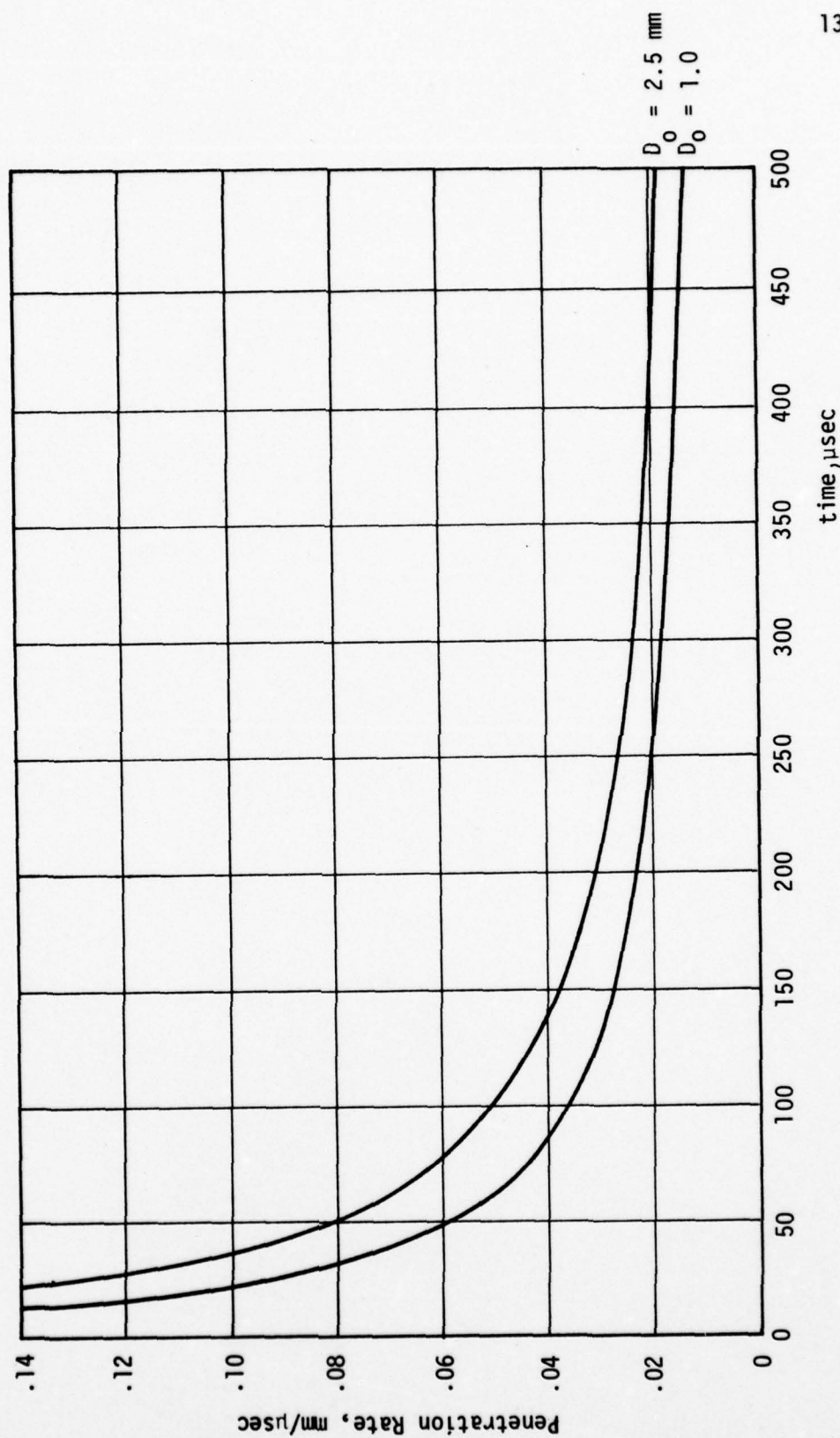
Figure 7.  Penetration Rate vs. Time, $\gamma = 1.2$, $T_0 = 3000°K$

13
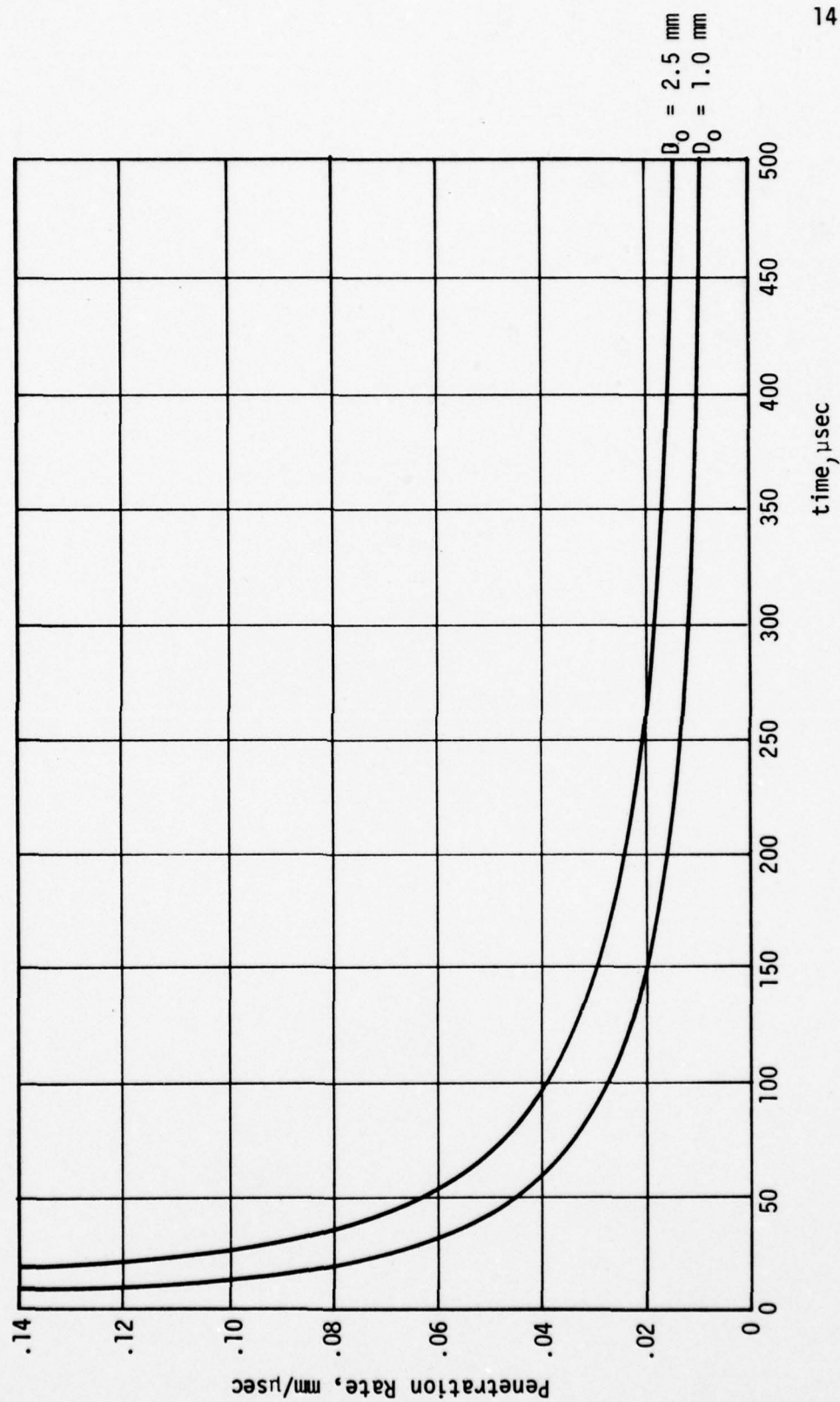
Figure 8. Penetration Rate vs. Time, $\gamma = 1.4$, $T_0 = 294°K$

14
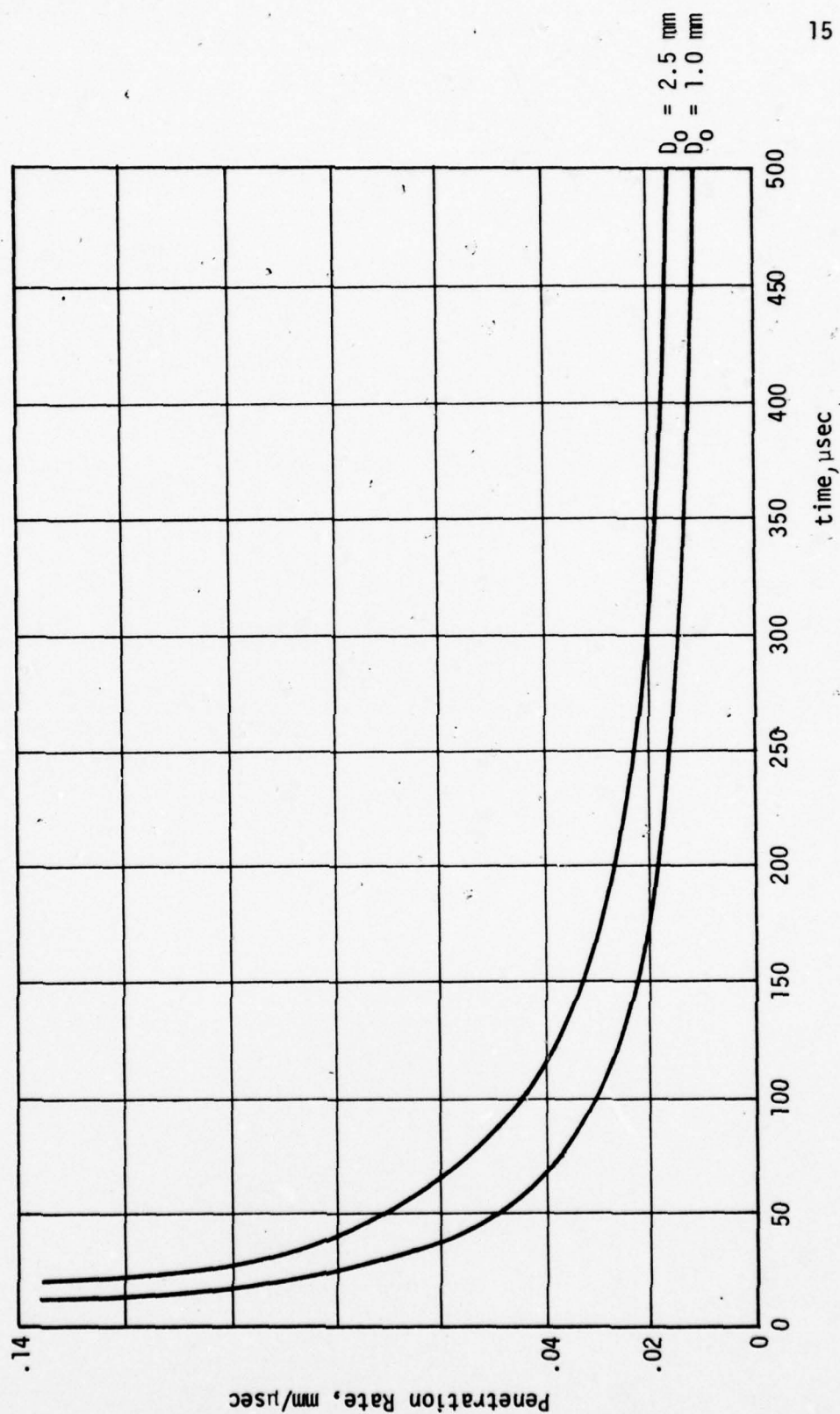
Figure 9.  Penetration Rate vs. Time, $\gamma = 1.4$, $T_0 = 1000°K$

15

## Experimental Effort

The experimental effort included the design, construction and testing of an apparatus for the simulation of the ignition phase. Figure 12 illustrates the primary injection cylinder. A mechanically sheared diaphram allowed control of the start of the gaseous injection into the liquid chamber for photographic purposes. Several materials were tested for use in the diaphram for repeatability. Aluminum disks were finally selected for the greatest repeatability. As the diaphram is sheared, the pieces and plug will necessarily have to have a cavity to fall into, thus increasing the volume above the plug, and reducing the pressure. By using different pin lengths, the pressure prior to diaphram rupture was controlled up to about 28000 psia, which was sufficient for a controlled design injection pressure of 200000 psia. Ballistics type piezoelectric pressure taps were used to monitor the pressure in the cylinder at all times during the injection sequence.

During a test, a high speed camera was used to observe bubble shape, injection distance and rate, and gas-liquid entrainment. Of primary interest was the sensitivity of geometry, gas type, injection velocities and upstream pressures on repeatability of the cavity formation. A square cross sectional liquid chamber was used to simplify the photography, although reflecting waves off this shape gave results somewhat different than what would occur for the cylindrical shape of a gun chamber. Future work could include piezocrystal monitoring of the square and round shapes to determine if there is any significant variations in results. If this is indicated, then a round section with appropriate optics could be developed for photographic purposes.

The experimental apparatus (shown in Figure 10) included a gas regulator, air filter, oil lubricator, solenoid switch, piston, 1/2 inch high pressure cylinder, water tank and gas supply system. The piston was made of cold roll stainless steel and was provided with two teflon o-rings to reduce gas leaks. The diaphrams (.048 and .078 inch) were designed to rupture at prescribed pressures, although in operation the rupture was controlled by a plunger at the end of the piston. The orifices were cut from brass (1mm & 2mm). Grease was used to block the orifice prior to each run to eliminate water seepage into the ullage upstream of the orifice. The water tank was of rectangular shape 8 x 1.25 x 1.25 inches and designed to withstand 2000 psia. Two piezo-electric crystals were used to measure pressure in the tank and one was placed in and fed into a four channel vertical amplifier oscilloscope containing a time base and delay generator. A polaroid camera was attached to the oscilloscope for impressions of pressure variations. A high speed camera was used to capture the injection sequence and had the capability of 11,000 frames per second, f of 1.9, zoom lense and usable distances of 4 to 100 feet. f of 4.0 was used for all tests and provided good resolution. The light source included two 1000 watts tungsten hallogen spotlights and three 500 watts super flood #2 photoflood bulbs. These light sources were kept about 1 foot from the tank. In order to get maximum light, one spot light and one super flood light were kept in between camera and tank. One spot light and two superflood lights were kept behind the water tank. Precaution was taken to prevent excessive light entering into camera, by shielding it with a black sheet. All of the lights were positioned at 45° angle with

the tank.

For pressure measurements peizo-electric crystals in the high pressure cylinder were calibrated at 500 psia per unit.  Crystals in the tank (upstream) were calibrated at 100 psia per unit. A single sweep mode was used per crystal.  On the time scale, one unit was one second.  The total length of travel of the beam was about 7 units, hence, from the instance the beam was triggered, it took about 7 seconds for the beam to go from one end to another.  The solenoid switch and camera motor was thus started within these seven seconds.

Figure 14 shows a typical pressure-time trace from the oscilloscope; this one from test case #1.  Trace (1) represents the pressure in the cylinder while trace (2) represents that of the liquid chamber.  For this case, the cylinder pressure increases rapidly from its initial pressure of 250 psia to 1450 psia just prior to diaphragm rupture.  A time lag is shown from the diaphragm rupture time to the increase in chamber pressure.

A frame by frame analysis provided the information for calculating the depth and rate of penetration for the cases run and are plotted in Figures 19 and 20.
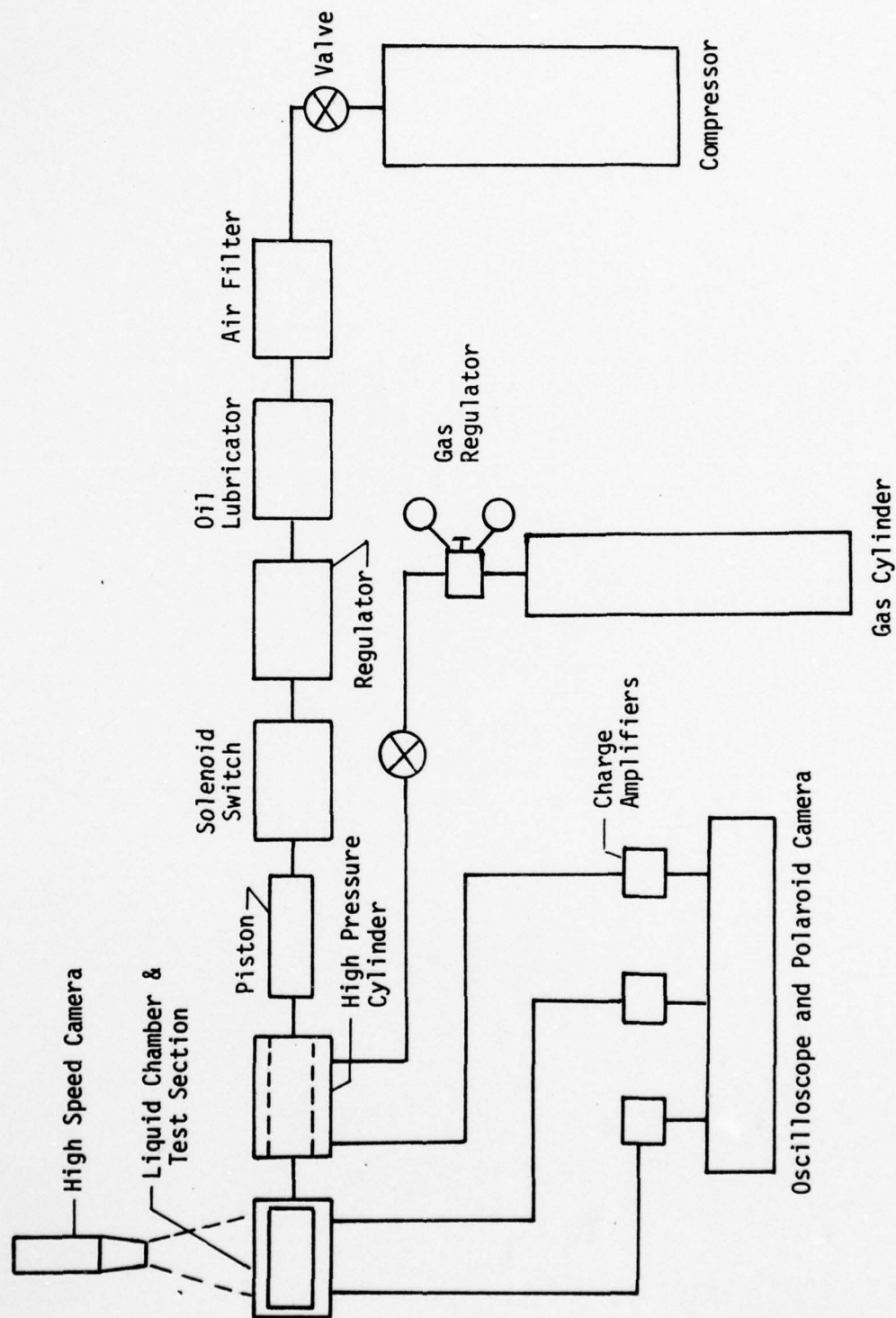
Figure 10. Schematic of Test Components and Arrangement
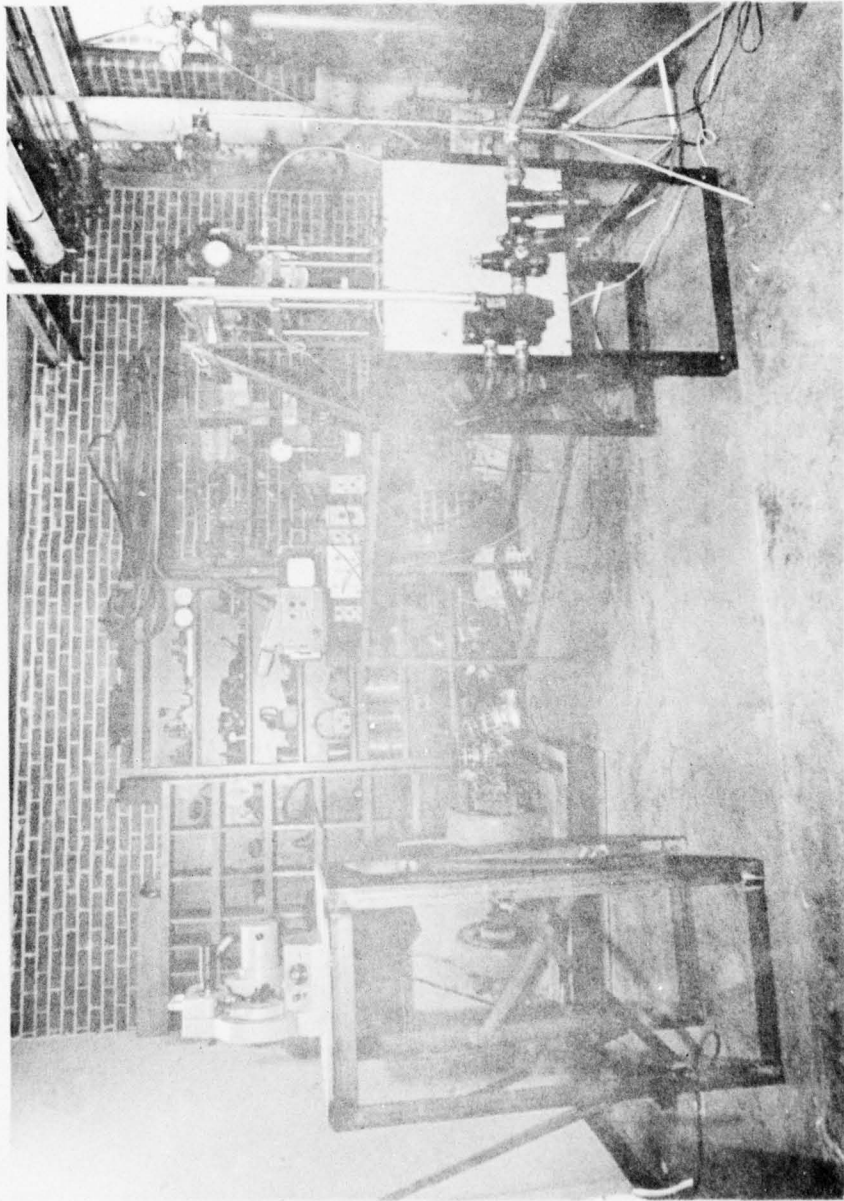
Figure 11. Photograph of Test Set-Up
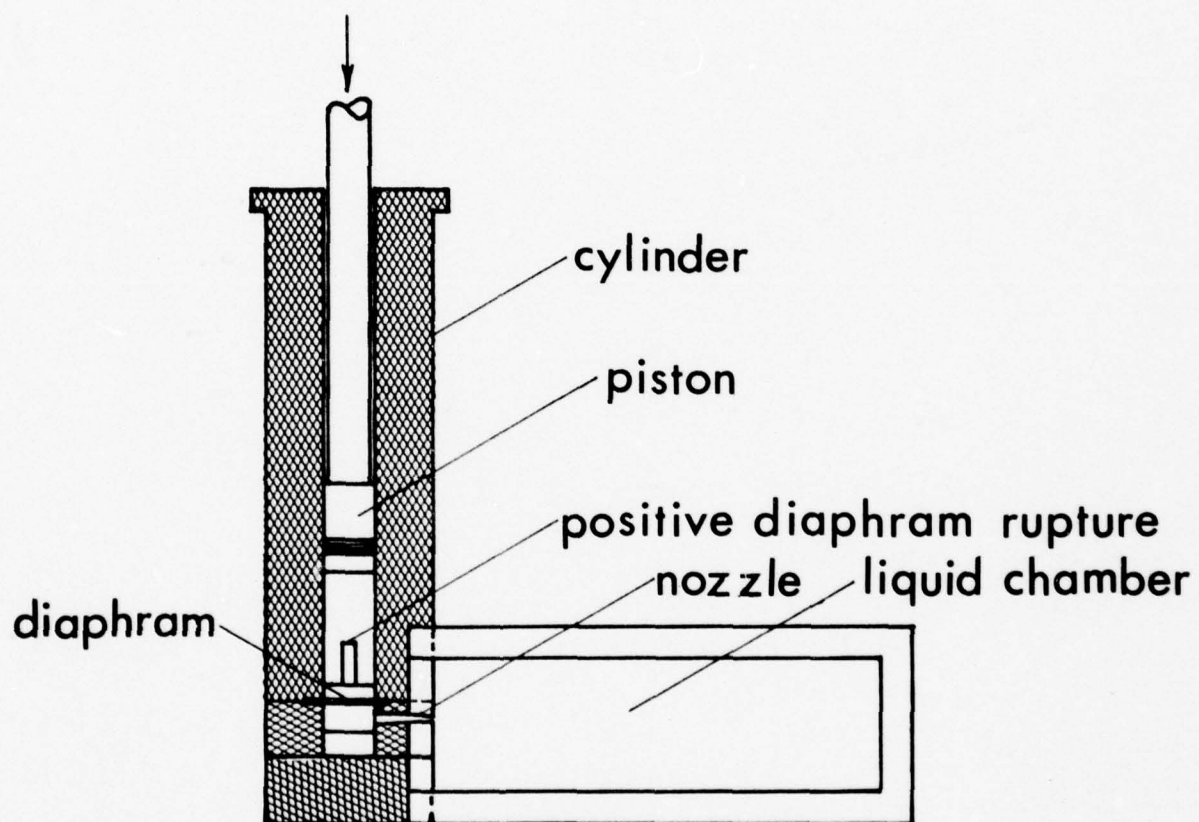
Figure 12. Primary Injection Cylinder Arrangement
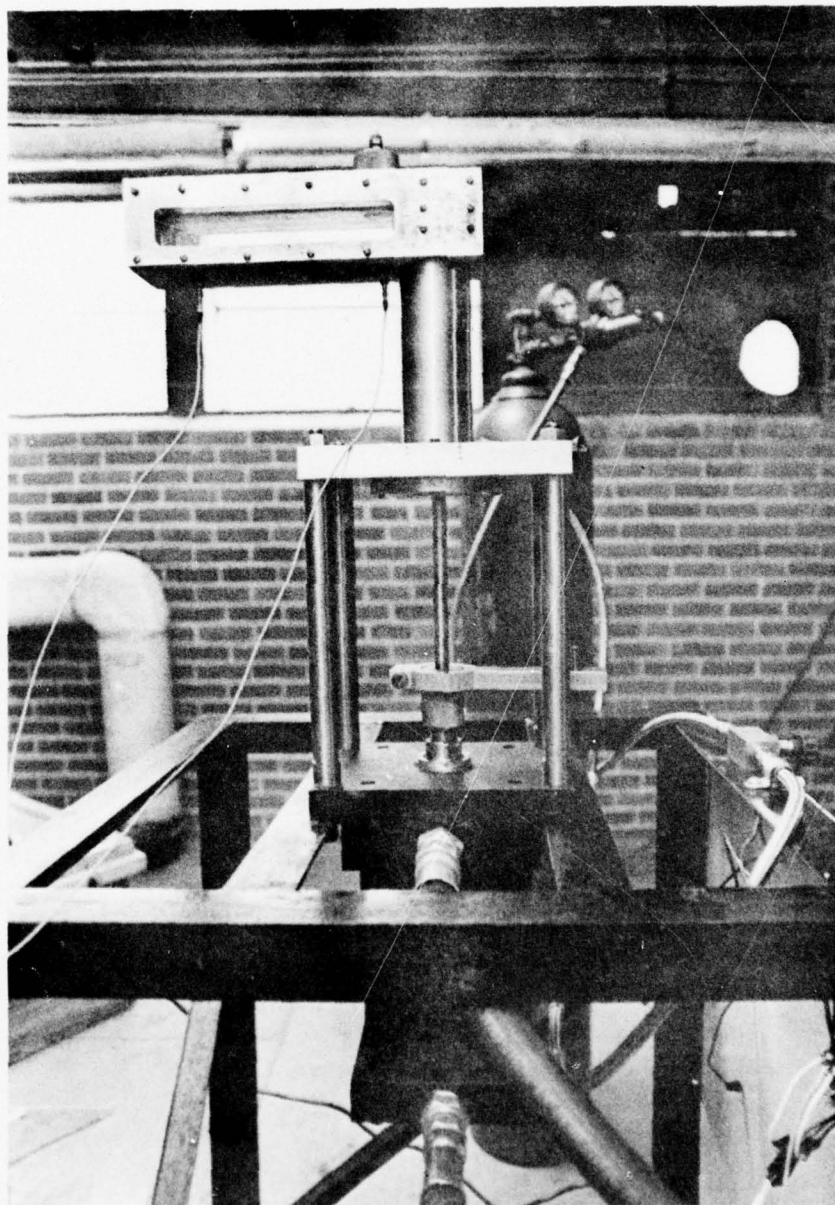
Figure 13.  Photograph of Test Stand
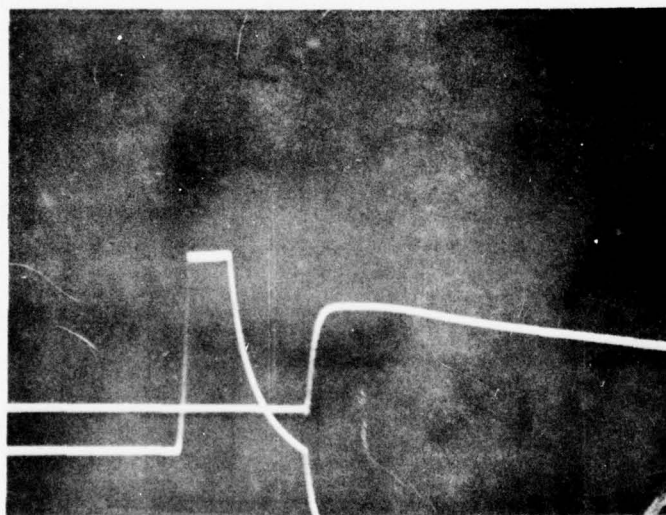
Figure 14.   Pressure-time curve from Oscilliscope

# Test Cases

| Test | #1 |
|---|---|
| $P_{cylinder\ initial}$ | =250 psia |
| $P_{cylinder\ final}$ | =1,350 psia |
| $P_{tank\ initial}$ | =14.5 psia |
| $P_{tank\ final}$ | =180 psia |
| Diameter | =1mm |
| PPS | =2000 |
| F | =1.73 |

| Frame No: | Time msec | Distance (Pictorial) | Distance (Actual) inches | Velocity Ft/sec |
|---|---|---|---|---|
| 1 | 0.5 | 6/32 | 0.324 | 54.06 |
| 2 | 1.0 | 12/32 | 0.649 | 54.06 |
| 3 | 1.5 | 16/32 | 0.865 | 37.5 |
| 4 | 2.0 | 20/32 | 1.08 | 34.45 |
| 5 | 2.5 | 23/32 | 1.24 | 27.07 |
| 6 | 3.0 | 26/32 | 1.40 | 27.07 |
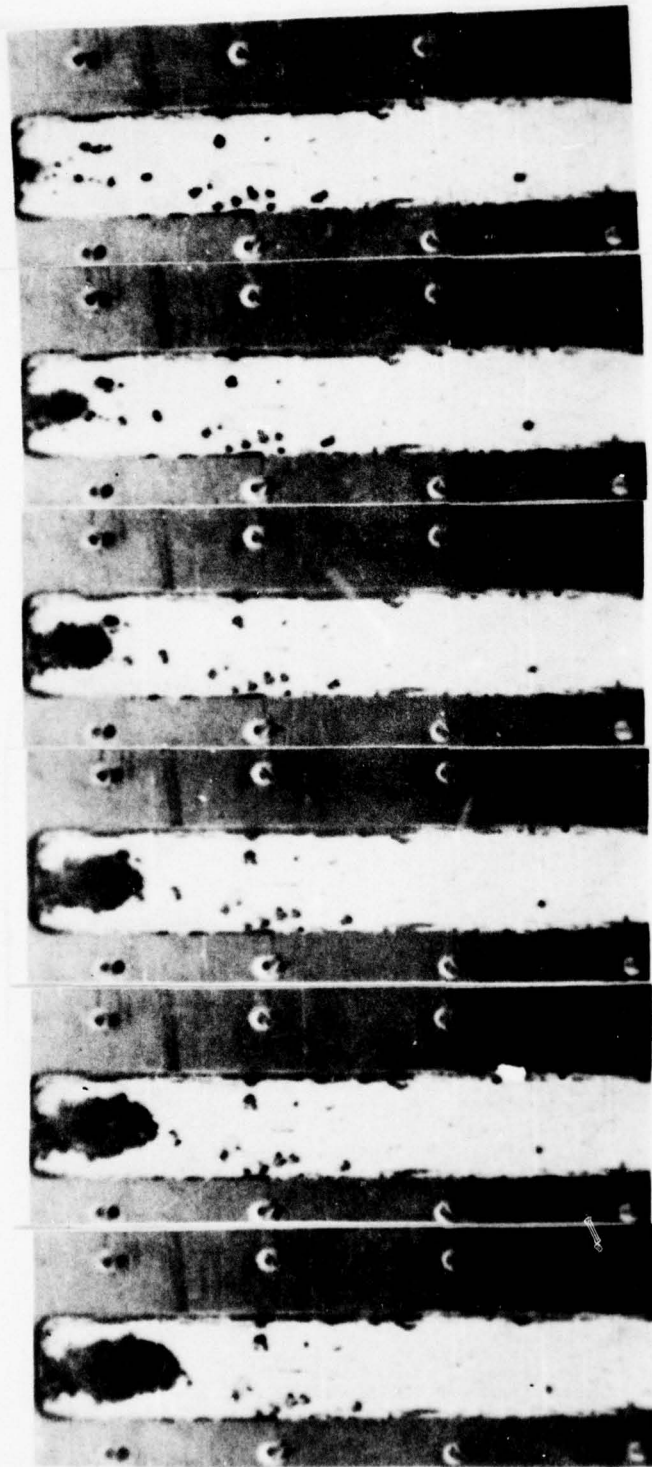
Time = 0.5 msec
Disp.= 0.324 inch
vel. = 54.06 ft/sec

Time = 1.0 msec
Disp.= 0.649 inch
Vel. = 54.06 ft/sec

Time = 1.5 msec
Disp.= 0.865 inch
Vel. = 37.5 ft/sec

Time = 2.0 msec
Disp.= 1.08 inch
Vel. = 34.45 ft/sec

Time = 2.5 msec
Disp.= 1.24 inch
Vel. = 27.07 ft/sec

Time = 3.0 msec
Dist.= 1.40 inch
Vel. = 27.07 ft/sec

Figure 15.  Photograph of Penetration Sequence
            Test Case #1

Test                     #2

$P_{cylinder}$ initial    =600 psia

$P_{cylinder}$ final      =2,600 psia

$P_{tank}$    initial    =14.5 psia

$P_{tank}$    final      =280 psia

Diameter                 =1mm

PPS                      =2,000

F                        =1.875

| Frame No: | Time msec | Distance (Pictorial) | Distance (Actual) inches | Velocity Ft/sec |
|---|---|---|---|---|
| 1 | 0.5 | 33/63 | .967 | 161.17 |
| 2 | 1.0 | 56/64 | 1.641 | 112.33 |
| 3 | 1.5 | 66/64 | 1.934 | 48.33 |
| 4 | 2.0 | 72/64 | 2.168 | 39.23 |
| 5 | 2.5 | 80/64 | 2.402 | 39.23 |
| 6 | 3.0 | 88/64 | 2.578 | 29.22 |
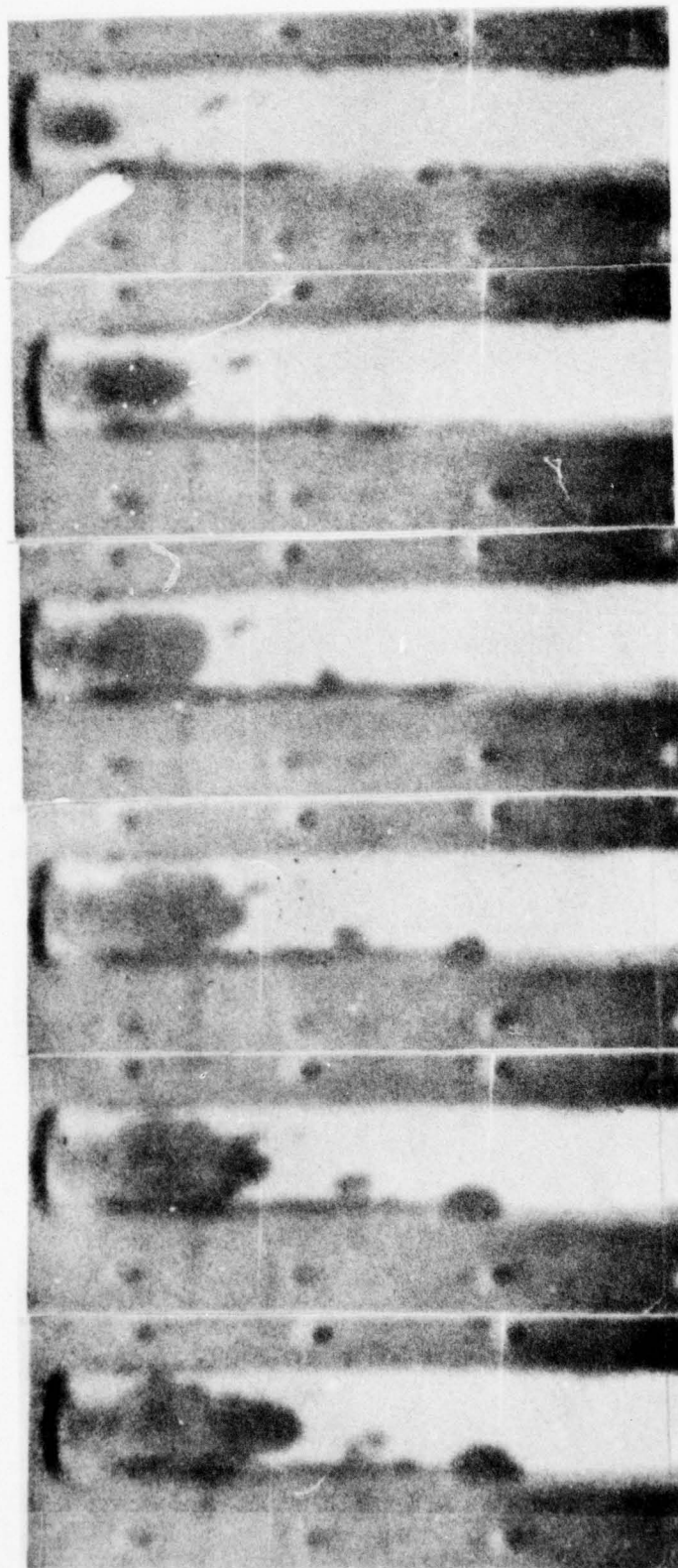
Time =      0.5    msec
Dist.=      0.967  inch
Vel. =    161.17   ft/sec

Time =      1.0    msec
Dist.=      1.641  inch
Vel. =    112.33   ft/sec

Time =      1.5    msec
Dist.=      1.934  inch
Vel. =     48.33   ft/sec

Time =      2.0    msec
Dist.=      2.168  inch
Vel. =     39.23   ft/sec

Time =      2.5    msec
Dist.=      2.402  inch
Vel. =     39.23   ft/sec

Time =      3.0    msec
Dist.=      2.578  inch
Vel. =     29.22   ft/sec

Figure 16.   Photograph of Penetration Sequence
Test Case #2

Test                       #3

$P_{cylinder}$ initial     =500 psia

$P_{cylinder}$ final       =2,500psia

$P_{tank}$     initial     =14.5 psia

$P_{tank}$     final       =260 psia

Diameter                   ≈2mm

F                          ≈1.915

| Frame No: | Time msec | Distance (Pictorial) | Distance (Actual) inches | Velocity Ft/sec |
|---|---|---|---|---|
| 1 | 0.67 | 20/32 | 1.197 | 149.63 |
| 2 | 1.33 | 33/32 | 1.975 | 97.25 |
| 3 | 2.00 | 41/32 | 2.45 | 59.75 |
| 4 | 2.67 | 47/32 | 2.81 | 44.94 |
| 5 | 3.33 | 52/32 | 3.11 | 37.31 |
| 6 | 4.00 | 56/32 | 3.35 | 30.00 |
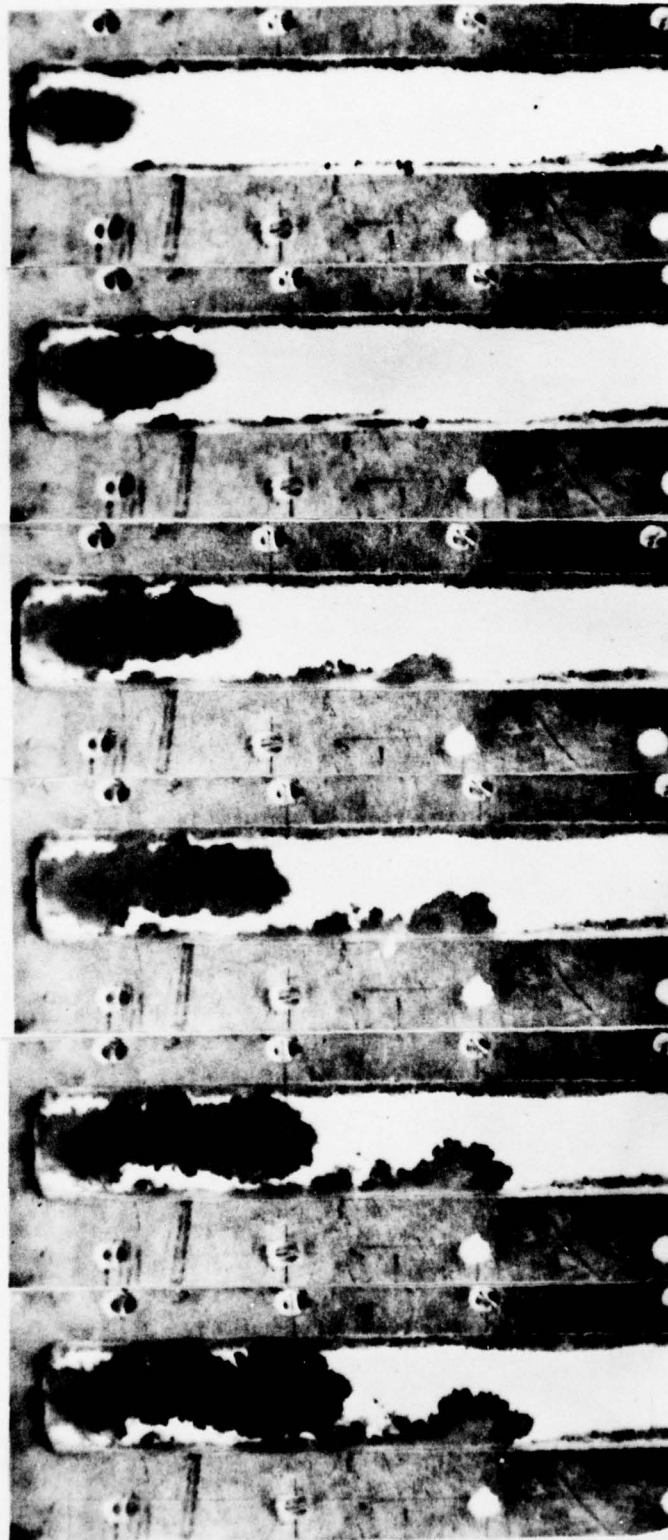
Time = 0.67 msec
Dist.= 1.197 inch
Vel. = 149.63 ft/sec

Time = 1.33 msec
Dist.= 1.975 inch
Vel. = 97.25 ft/sec

Time = 2.00 msec
Dist.= 2.45 inch
Vel. = 59.73 ft/sec

Time = 3.33 msec
Dist.= 3.11 inch
Vel. = 37.31 ft/sec

Time = 2.67 msec
Dist.= 2.81 inch
Vel. = 44.94 ft/sec

Time = 4.0 msec
Dist.= 3.35 inch
Vel. = 30.00

Figure 17.   Photograph of Penetration Sequence
            Test Case #3

Test                           #4

$P_{cylinder\ initial}$        =1,000 psia

$P_{cylinder\ final}$          =5,000 psia

$P_{tank\ initial}$            = 14.5 psia

$P_{tank\ final}$              =500   psia

Diameter                       =2mm

PPS                            =3,000

F                              =1.957


| Frame No: | Time msec | Distance (Pictorial) | Distance (Actual) inches | Velocity Ft/sec |
|---|---|---|---|---|
| 1 | 0.33 | 46/64 | 1.40 | 350.0 |
| 2 | 0.67 | 76/64 | 2.32 | 230.8 |
| 3 | 1.00 | 91/64 | 2.78 | 114.8 |
| 4 | 1.33 | 104/64 | 3.18 | 99.3 |

Time =      0.33  msec
Dist.=      1.40  inch
Vel. =    350.0   ft/sec


Time =      0.67  msec
Dist.=      2.32  inch
Vel. =    230.8   ft/sec


Time =      1.00  msec
Dist.=      2.78  inch
Vel. =    114.8   ft/sec


Time =      1.33  msec
Dist.=      3.18  inch
Vel. =     99.30  ft/sec

Figure 18.   Photograph of Penetration Sequence
             Test Case #4
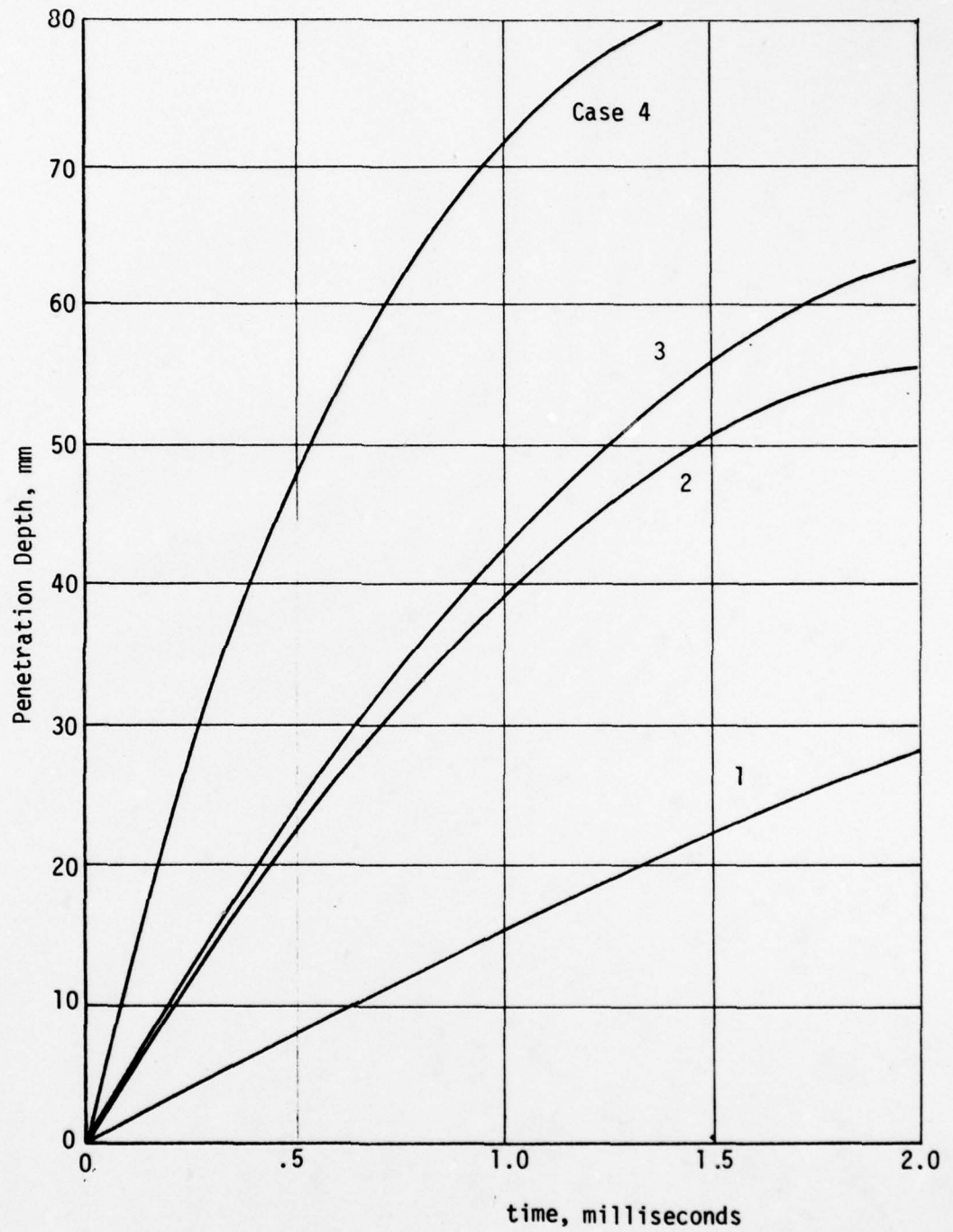
Figure 19. Penetration Depth for Cases as a Function of Time
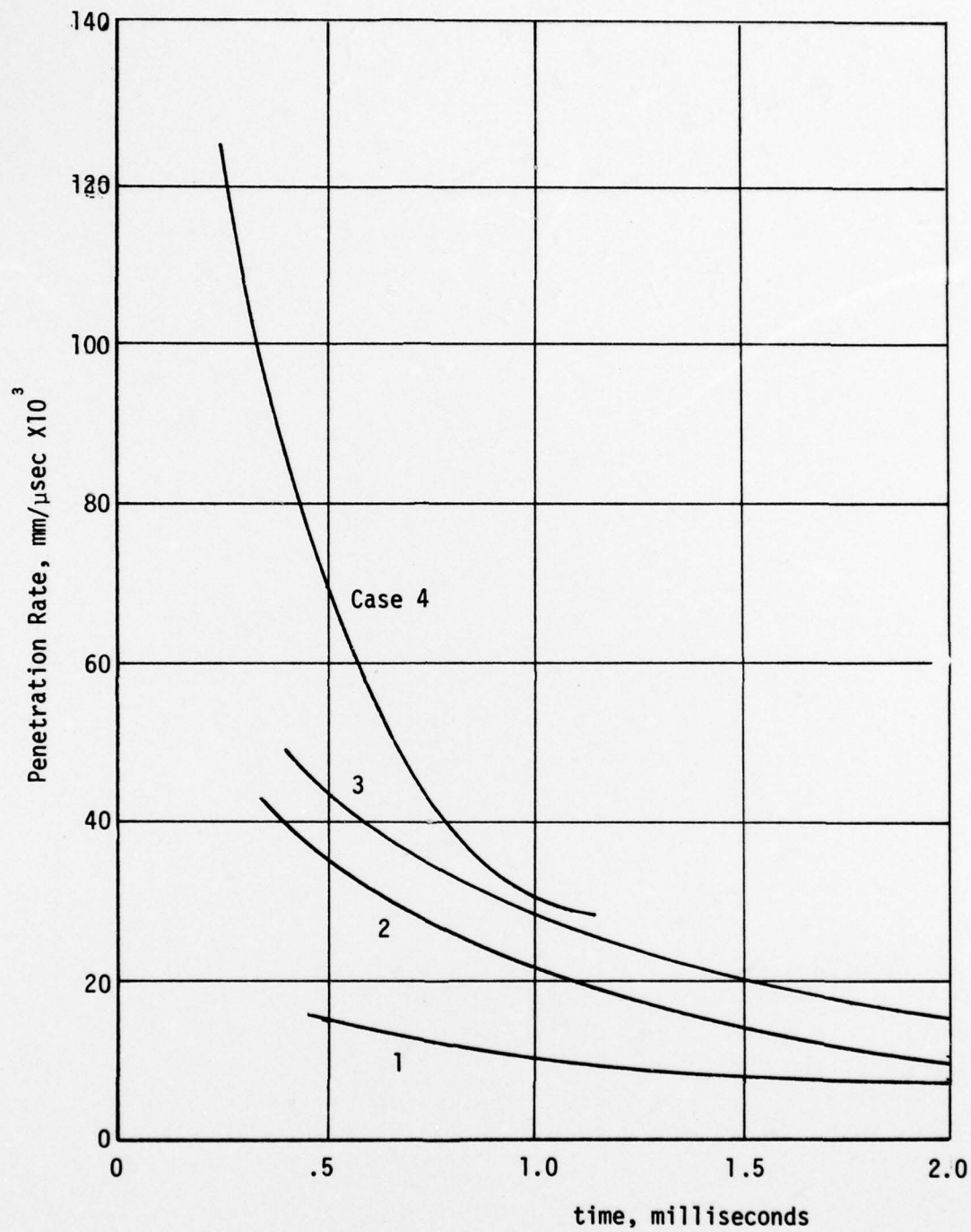
Figure 20.   Penetration Rate for Cases as
a Function of Time

## Conclusions

Simulation of the penetration sequence for gaseous injections into liquid propellants provided greater understanding of the significants of geometry and flow conditions on gas bubble formation, penetration depth and rate. Comparisons of test data and the simulation model indicated that the model is good to excellent in predicting the penetration depth and rate of the injection for the first 500 micro-seconds. The shape of the bubble obtained experimentally approached closely to the prolate spheroid assumed for model I. The excellent agreement between the test data and simulation program also provided support for the assumptions made for the program.

## REFERENCES

1. J. W. DeDapper, T. P. Goebel and R. A. Nagy, "Observations on the Behavior of Pyrotechnic Primers," Sixth Annual Conference in the Application of LP to Guns, June, 1955.

2. J. E. Regan and C. Shabelan, "Ignition Studies of Liquid Monopropellants for Guns," Frankford Arsenal Report Number 1288, October 1955.

3. R. H. Comer, R. B. Shearer and R. N. Jones, "Interior Ballistics of Liquid Propellant Guns," Ballistic Research Laboratories Report Number 1205, May 1963.

4. R. H. Comer, R. N. Jones, and R. B. Shearer, "Predicted Performance of a High Pressure, High Velocity Liquid Propellant Gun (U)," Ballistic Research Laboratories Memorandum Report Number 1573, July 1964, (Confidential).

5. R. N. Jones, R. H. Comer, R. B. Shearer and L. Stansbury, " A Source of Variability in the Interior Ballistics of Liquid Propellant Guns," Ballistic Research Laboratories Report Number 1288, June 1965.

6. A. C. Haukland, "State-of-the-Art Survey of Liquid Propellant Gun System," U. S. Naval Ordnance Station Report IHTR 350, December, 1971.

7. W. F. McBratney, I. C. Stobie, J. D. Knapton, and R. H. Comer, "Liquid Propellant Gun Program, Progress Report, BRL IMR 231, May, 1974.

8. R. A. Hartmen, J. D, Knapton, I. C. Stobie and R. H. Comer, "A Study on the Establishment of a Pyrotechnic Ignition Criteria for Liquid Propellant Guns,"BRL Report, April, 1975.

9. J. D. Knapton, et al, "Survey of Ballistics Data from High Velocity Liquid Propellant Gun Firings", BRL R 2005, August 1977.

10. C. R. Wimberly, "Some Observations on the Ignition Systems used on Liquid Propellant Guns," Research Report, U.S. Army BRL. August 1975.

11. C. R. Wimberly, "An Investigation of High Pressure Gaseous Injections into Liquid Propellants", Research Proposal to the ARO, August, 1976.

12. A. R. Guzdar, S. S. Rhee and A. J. Erickson, "Modeling Studies of the Liquid Propellant Guns (U)," Ballistic Research Laboratories Contract Report No. 57, October 1971, (Confidential).

13. R. H. Comer and W. F. McBratney, "Transient Combustion Modeling in Bulk Loaded Liquid Monopropellant Guns (U)," 9th JANNAF Combustion Meeting, Vol 111, Chemical Propulsion Information Agency, pp. 71-99, September 1972, (Confidential).

14. J. S. Howland, S. S. Rhee, A. J. Erickson and A. R. Guzdar, "A Study of the Hydrodynamic Aspects of the Physical Processes in Liquid Propellant Guns (U)," Final Report, Foster-Miller Associates, Inc., Waltham, Massachusetts, November 1968, (Confidential).

15. E. L. Lee and H. C. Hornig, "Equation of State of Detonation Product Gases," Proceedings from the Twelfth International Conference on Combustion, Pittsburg, Pennsylvania, 1969.

16. R. H. Comer and W. F. McBratney, "Transient Combustion Modeling in Bulk Loaded Liquid Monopropellant Guns," presented at the 9th JANNAF Combustion Meeting, Naval Post Graduate School, Monterey, California, September, 1972.

17. S. G. Mikhlin and K. L. Smolitskig, "Approximate Methods for Solution of Differential and Intergral Equations", Vol. 5, Modern Analytic and Computational Methods in Science and Mathematics, Elsevier, N.Y. 1967 (pp. 263-268)

18. W. G. Soper, "Ingition Waves In PYRO Propellant," Combustion and Flame 20, pp. 157-162, 1973.

19. W. G. Soper, "Ignition Waves in PYRO Propellant," Combustion and Flame 22, pp. 273-276, 1974.

20. M. Cowperthwaite, "Two-Dimensional Steady-State Detonation Waves," Proceedings from the Thirteenth International Symposium on Combustion," Pittsburg, Pennsylvania, 1971.

21. W. F. McBratney, B. D. Bensinger and W. B. Alford, "Strand Combustion Rates for Some Liquid Monopropellants at Gun Functioning Pressure", BRL MR 2658, August, 1976.

22. J. H. Littlefair and G. W. Stock, "Fuseless Strand Burning Methods for the Measurement of Rates of Burning of Solid Propellants and of Liquid Monopropellants," ERDE TN 40, September 1971.

23. O. C. Zienkiewicz and C. Taylor, "Weighted Residual Processes in Finite Element Method With Particular Reference to Some Transient and Coupled Problems," Lectures on Finite Element Methods in Continuum Mechanics, U. of Alabama Press, Huntsville, Ala. 1973.

24. P. Hood, " A Finite Element Solution of the Navier-Stokes Equations for Incompressible Contained Flow", M. S. Thesis, U. of Wales, Swansea, U.K., 1970.

25. G. Hiriart and T. Sarpkaya, "Jet Impingement on Axisymmetric Curved Deflectors," Proceeding International Symposium on the Finite Element Method in Flow Problems, University College of Wales, Swansea, 1974.

APPENDIX  -  PROGRAM LISTING

```
C
C
C       PROGRAM FOR ANALYSIS OF LIQUID PROPELLANT GUNS
C
C
        COMMON V0,A,B,GEC,A1,A2,A3,VL,VG,GAM,T0,TEMP,KEY,DP,
     1  AREA,CL,KEY2,P0
        DIMENSION RATIO(10), AXIS(10,200),AXMIN(10,200)
        DIMENSION VOLG(200),VOLL(200),PRESS(200),TIME(200),STEMP(200)
C
C
C       INPUT GEOMETRY PARAMETERS
C
        READ (2,1) D0,CD,CL
     1  FORMAT(4E)
C
C
C       INPUT GAS PARAMETERS
C
        READ (2,1) GAM,R,P0,Z0,A1,A2,A3,T0
C
C
C       INPUT LIQUID PARAMETERS
C
        READ(2,1)A,B,C
C
C
C       INPUT TIME PARAMETERS
C
        READ (2,1) DT,TF
C
C
C       INPUT PROLATE SPHEROID PARAMETERS
C       RATIO = MINOR DIAMETER/MAJOR DIAMETER
C       N = NUMBER OF RATIOS TO BE CONSIDERED
C
        READ (2,2) N
     2  FORMAT(I)
C
C
C       DATA CHECK
C
        WRITE(3,4)D0,CD,CL
     4  FORMAT('1',3E16.8)
        WRITE(3,5)GAM,R,P0,Z0,A1,A2,A3,T0
     5  FORMAT(1X,4E16.8)
        WRITE(3,6)A,B,C,DT,TF,N
     6  FORMAT(1X,5E16.8,I5/'1')
C
C
C       CONVERT INPUT DATA
C
        D0=D0/(25.4*12.)
        R=R*1545.33/8314.5
        P0=P0/6.8948E3
        T0=T0*9./5.
        A0=3.14159*D0*D0/4.
        DM=(2./(GAM+1.))**((GAM+1.)/(GAM-1.))
        DM=SQRT(GAM*32.174*DM/R)
        DL=DM*A0*P0*144./(Z0*SQRT(T0))
        DT=DT*1.E-6
        TF=TF*1.0E-6
        CD=CD/(25.4*12.)
        C=C/(25.4*12.)
        CL=CL/(25.4*12.)
        AREA=3.14159*CD*CD/4.
C
C
C       INPUT SHAPE FACTORS
C
        DO 100 J=1,N
```

```
100     READ (2,1) (ATIG(I)
        KEY = 1
        KEY1=0
C
C       PHASE 1 - WAVE MOVING DOWNSTREAM - KEY = 1
C       PHASE 2 - WAVE MOVING UPSTREAM - KEY = 2
C       PHASE 3 - WAVE MOVING DOWNSTREAM - 2ND TIME - KEY = 3
C       PHASE 4 - WAVE MOVING UPSTREAM - 2ND TIME - KEY = 4
C
        P1=0.
        NF=TF/DT+3.
        NT=(CL/C)/DT+1.
        NT1=NT
        T=0.
        PD=0.
        DO 101 J=1,NF
        IP2=1
144     T=T+DT
        IF(T.LE.(TF+0.5E-6))GOTO149
        NG=J-1
        GO TO 117
149     IF(J.EQ.NT)GOTO112
        IF(J.NE.(NT+1))GOTO111
        IF(KEY.NE.1)GOTO121
        AT=NT
        T=AT*DT
        KEY=2
        NT=(2.*CL/C)/DT+2.
        DT=P1
        VO=AREA*(CL-C*(T-CL/C))
        GO TO 114
121     IF(KEY.NE.2)GOTO122
        AT=NT+NTF
        T=AT*DT
        KEY=3
        KEY1=0
        NT=(3.*(CL/C-T)/DT+1.
        NT=NT+J
        NT3=NT
        VO=AREA*C*(T-2.*CL/C)
        GO TO 114
122     T=TSAVE
        KEY=4
        KEY1=0
        VO=AREA*(CL-C*(T-3.*CL/C))
        GOTO114
112     IF(KEY.NE.1)GOTO123
        T=CL/C
        VO=AREA*C*T
        GO TO 114
123     IF(KEY.LE.2)GOTO124
        T=2.*CL/C
        VO=AREA*CL
        KEY1=1
        GO TO 114
124     TSAVE=T
        T=3.*CL/C
        KEY1=1
        VO=AREA*CL
        GO TO 114
111     IF(KEY.NE.1)GOTO125
```

THIS PAGE IS BEST QUALITY PRACTICABLE
FROM COPY FURNISHED TO DDC

```
      VO=AREA*C*T
      GO TO 114
125   IF(KEY.NE.2)GOTO126
      VO=AREA*(CL-C*(T-CL/C))
      GOTO114
126   IF(KEY.NE.3)GOTO127
      VO=AREA*C*(T-2.*CL/C)
      GO TO 114
127   VO=AREA*(CL-C*(T-3.*CL/C))
114   GMC=DM*R*(T-0.5*5.0E-6)
      IF(T.LT.5.0E-6)GMC=DM*R*0.5*(DM/5.0E-6)*T**2
C
C     SEARCH FOR APPROXIMATE LOCATION OF ROOT
C     PRFNC = FUNCTION OF PRESSURE SET EQUAL TO ZERO
C
152   F1=PRFNC(P1)
      IF(F1.LT.0.)GO TO 151
      P1=P1-50.
      IF(P1.GT.0.)GO TO 152
      WRITE (3,154) P1,F1
154   FORMAT('0',5X,'NEGATIVE PRESSURE'/6X,'P1 =',E16.8,5X,
     1 'F1 =',E16.8)
      NF=J
      GO TO 117
151   P2=P1
150   P2=P2+100.
      IF(P2.LT.10000)GOTO141
C
C     IF PRESSURE EXCEEDS 10,000 PSI IN TIME INCREMENT
C     DT IS HALVED 4 TIMES
C
      IP2=IP2+1
      IF(IP2.LT.5)GOTO142
      WRITE(3,143)DT
143   FORMAT('0',10X,'PRESSURE EXCEEDS 10,000 PSI IN TIME INCREMENT =',
     1 E18.8)
      NF=J
      GO TO 117
142   DT=DT/2.
      GO TO 144
141   F2=PRFNC(P2)
      IF(F2.LT.0.)GO TO 150
C
C     HALF FINDS PRESSURE - SETS IT EQUAL TO P1
C
      CALL HALF(P1,P2,F1)
C
C     FIND MAJOR AND MINOR AXES OF PROLATE SPHEROID
C
      DO 102 I=1,N
      AXIS(I,J)=((3.*VG)/(4.*3.14159*RATIO(I)**2))**(1./3.)
      AXIS(I,J)=AXIS(I,J)*12.*25.4
      AXMIN(I,J)=RATIO(I)*AXIS(I,J)
      IF(KEY.NE.2)GOTO102
      IF(KEY1.EQ.1)GOTO102
      IF(AXIS(I,J).GE.((CL-C*(T-CL/C))*12.*25.4))KEY=9
102   CONTINUE
      VOLG(J)=VG*1728.*25.4**3
      VOLL(J)=VL*1728.*25.4**3
      PRESS(J)=P1*6.8948E3
      TIME(J)=T
```

```
          STEMP(J)=TEMP*5./9.
          IF(KEY.NE.9)GOTO101
          NT=J+1
          NT2=NT
          NTF=(2.*CL/C-T)/DT+1.
          KEY=2
  101     CONTINUE
C
C         OUTPUT RESULTS
C
  117     WRITE(3,7)
    7     FORMAT(40X,'LIQUID PROPELLANT GUN'//)
          WRITE (3,8)
    8     FORMAT(44X,'BUBBLE GROWTH'///)
          WRITE (3,9)
    9     FORMAT(8X,'TIME',9X,'BREECH PRESSURE'  ,3X,'PROJECTILE PRESSURE',
     1    3X,'MAJOR AXIS',5X,'PRESSURE FRONT',6X,'GAS VOLUME',
     2    7X,'TEMPERATURE')
          WRITE(3,10)
   10     FORMAT(3X,'(MICRO SECONDS)',6X,'(PASCALS)',11X,'(PASCALS)',
     1    11X,'(MM)',13X,'(MM)',12X,'(CU MM)',11X,'(DEG-K)'//)
          DP=DP*6.8948E3
          TO=TO*5./9.
          DO 103 I=1,I
          WRITE (3,11) RATIO(I)
   11     FORMAT('0',50X,'RATIO =',F7.4)
          T=0.
          WRITE(3,12) T,T,T,T,T,T,TO
   12     FORMAT(7(2X,E16.8))
          DO 104 K=1,IG
          IF(K.GT.NT1)GOTO131
          PF=C*TIME(K)*12.*25.4
          PL=0.
          GO TO 139
  131     IF(K.GT.NT2)GOTO132
          PF=(CL-C*(TIME(K)-CL/C))*12.*25.4
          PL=PRESS(K)+DP
          GO TO 139
  132     IF(K.GT.NT3)GOTO133
          PF=C*(TIME(K)-2.*CL/C)*12.*25.4
          PL=PRESS(K)-DP
          GO TO 139
  133     PL=(CL-C*(TIME(K)-3.*(L/C))*12.*25.4
          PL=PRESS(K)+DP
  139     TIME(K)=TIME(K)*1.E6
          WRITE(3,12)TIME(K),PRESS(K),PL,AXIS(I,K),PF,VOLG(K),STEMP(K)
          IF(K.EQ.NT1)WRITE(3,13)
          IF(K.EQ.NT2)WRITE(3,14)
          IF(K.EQ.NT3)WRITE(3,13)
   13     FORMAT('0',20X,'PRESSURE WAVE REACHES PROJECTILE BASE'//)
   14     FORMAT('0',20X,'PRESSURE WAVE REACHES BREECH END'//)
  104     CONTINUE
  103     CONTINUE
          STOP
          END
          FUNCTION PRENC(P)
C
C         CALCULATES PRESSURE FUNCTION
C         TOTAL VOLUME  =  LIQUID VOLUME + GAS VOLUME
C
          COMMON V0,A,B,GEC,A1,A2,A3,VL,VG,GAM,TO,T,KEY,DP,
```

```
      1    AREA,CL,KEYZ,VO
           Z=A1+A2*P+A3*P*P
           IF(Z.LT.1.)Z=1.
           PA=P+14.7
           T=TO*(PA/PO)**((GAM-1.)/GAM)
           IF(KEY.EQ.1)GOTO1
           IF(KEY1.EQ.1)GOTO1
           V1=AREA*CL-VO
           IF(KEY.EQ.3)DP=-DP
           VTMP=((A+B*(P+DP))/A)**(-1./B)
           IF(KEY.EQ.3)DP=-DP
           VL1S=V1/VTMP
           VLOS=VO+V1-VL1S
           VTMP=((A+B*P)/A)**(-1./B)
           VL=VLOS*VTMP
           GO TO 2
      1    VL=VO*((A+B*P)/A)**(-1./B)
      2    VG=GMC*Z*T/(PA*144.)
           PREHC=VL+VG
           PRELC=VO-PREHC
           RETURN
           END
           SUBROUTINE HALF(X1,X2,X)
C
C          CALCULATES ROOT BY HALF INTERVAL METHOD
C          SEE P175 - SOUTHWORTH & DELEEUW
C
           F1=X
      5    X=(X1+X2)/2.
           FM=PRINC(X)
           IF(F1*FM)1,2,3
      1    X2=X
           GO TO 4
      3    F1=FM
           X1=X
      4    IF((X2-X1).GT.1.0)GO TO 5
      2    RETURN
           END
```